

1  
2 ***Fendrr* synergizes with Wnt signalling to regulate fibrosis related genes during lung**  
3 **development**

4  
5  
6 Tamer Ali<sup>1,2,\*</sup>, Sandra Rogala<sup>1,\*</sup>, Maria-Theodora Melissari<sup>1</sup>, Sandra Währisch<sup>3</sup>, Bernhard  
7 G Herrmann<sup>3</sup> and Phillip Grote<sup>1,4\*\*</sup>

8  
9  
10  
11 <sup>1</sup> Institute of Cardiovascular Regeneration, Centre for Molecular Medicine, Goethe  
12 University, Theodor-Stern-Kai 7, 60590 Frankfurt am Main, Germany

13 <sup>2</sup> Faculty of Science, Benha University, Benha 13518, Egypt

14 <sup>3</sup> Department of Developmental Genetics, Max Planck Institute for Molecular Genetics,  
15 Ihnestr. 63-73, 14195 Berlin, Germany

16 <sup>4</sup> Georg-Speyer-Haus, Paul-Ehrlich-Str. 42-44, 60596 Frankfurt am Main

17  
18 \* Equal contribution

19 \*\* correspondence: [ph.grote@georg-speyer-haus.de](mailto:ph.grote@georg-speyer-haus.de)

20  
21 **RESEARCH ARTICLE**

22  
23  
24  
25 **KEYWORDS**

26 LncRNA, *Fendrr*, triplex, lung development, Wnt, fibroblasts  
27  
28  
29  
30  
31

32           **Abstract**

33   Long non-coding RNAs are a very versatile class of molecules that can have important  
34   roles in regulating a cells function, including regulating other genes on the transcriptional  
35   level. One of these mechanisms is that RNA can directly interact with DNA thereby  
36   recruiting additional components such as proteins to these sites via a RNA:dsDNA triplex  
37   formation. We genetically deleted the triplex forming sequence (*FendrrBox*) from the  
38   lncRNA *Fendrr* in mice and find that this *FendrrBox* is partially required for *Fendrr* function  
39   *in vivo*. We find that the loss of the triplex forming site in developing lungs causes a  
40   dysregulation of gene programs, associated with lung fibrosis. A set of these genes  
41   contain a triplex site directly at their promoter and are expressed in fibroblasts. We find  
42   that *Fendrr* with the Wnt signaling pathway regulates these genes, implicating that *Fendrr*  
43   synergizes with Wnt signaling in lung fibrosis.

44

45           **Introduction**

46   The number of loci in mammalian genomes that produce RNA that do not code for proteins  
47   is higher than the number of loci that produce protein coding RNAs (Ali and Grote, 2020;  
48   Hon et al., 2017). These non-protein coding RNAs are commonly referred to long non-  
49   coding RNAs (lncRNAs) if their transcript length exceeds 200 nucleotides. Many of these  
50   lncRNA loci are not conserved across species. However, some loci are conserved on the  
51   syntenic level and some even on the transcript level. One of the syntenic conserved  
52   lncRNAs is the *Fendrr* gene, divergently expressed from the essential transcription factor  
53   coding gene *Foxf1*. Both genes have been implicated in various developmental processes  
54   (Grote et al., 2013; Mahlapuu et al., 2001; Yu et al., 2010) and particularly in heart and  
55   lung development (Herriges et al., 2014; Sauvageau et al., 2013; Stankiewicz et al., 2009;  
56   Szafranski et al., 2013).

57   The *Fendrr* lncRNA was shown to be involved in several pathogeneses with fibrotic  
58   phenotypes. In a transverse aortic constriction (TAC) mouse model, *Fendrr* was  
59   upregulated in heart tissue. Loss of *Fendrr* RNA via an siRNA approach alleviated fibrosis  
60   induced by TAC, demonstrating a pro-fibrotic function for *Fendrr* in the heart (Gong et al.,  
61   2020). In contrast, in humans with Idiopathic Pulmonary Fibrosis (IPF) and in mice with  
62   bleomycin-induced pulmonary fibrosis, the *Fendrr/FENDRR* RNA was downregulated  
63   (Huang et al., 2020). In addition, depletion of *FENDRR* increases cellular senescence of  
64   human lung fibroblast. While overexpression of human *FENDRR* in mice reduced  
65   bleomycin-induced lung fibrosis, revealing an anti-apoptotic function of *FENDRR* in lungs  
66   and a conservation of the mouse *Fendrr* and the human *FENDRR* in this process.  
67   *Fendrr/FENDRR* seems to have opposing functions on fibrosis in heart and in lung tissue,  
68   indicating that secondary cues such as active signaling pathways might be required.

69   In the lung, *FENDRR* is a potential target for intervention to counteract fibrosis and the  
70   analysis of its function in this process and how target genes are regulated is of interest to  
71   develop RNA-based therapies (Polack et al., 2020). lncRNAs can exert their function on  
72   gene regulation via many different mechanisms (Melissari and Grote, 2016). One  
73   mechanism is that the RNA is tethered to genomic DNA either by base-pairing or by  
74   RNA:dsDNA triplex formation involving Hoogsteen base pairing (Li et al., 2016). Here, we  
75   deleted such a Triplex formation site in the *Fendrr* lncRNA *in vivo*. We identified genes

76 that are regulated by *Fendrr* in the developing mouse lung and require the triplex forming  
77 RNA element, which we termed the *FendrrBox*. The gene network that is regulated by  
78 *Fendrr* and require the *FendrrBox* element is associated with extracellular matrix  
79 deployment and with lung fibrosis. We verified that regulation of these genes is depending  
80 on the presence of full length *Fendrr* and active Wnt signaling, establishing that *Fendrr*,  
81 and, in particular, its *FendrrBox* element, is involved in Wnt dependent lung fibrosis.

82

83           **Results**

84   **The *FendrrBox* region is partially required for *Fendrr* RNA function**

85   We established previously that the long non-coding RNA *Fendrr* is an essential lncRNA  
86   transcript in early heart development in the murine embryo (Grote et al., 2013). In addition,  
87   the *Fendrr* locus was shown to play a role in lung development (Sauvageau et al., 2013).  
88   Expression profiling of pathological human lungs revealed that FENDRR is dysregulated  
89   in disease settings (for review see Xiao et al., 2017). In the second to last exon of the  
90   murine *Fendrr* lncRNA transcript resides a UC-rich low complexity region of 38bp, which  
91   can bind to target loci and thereby tether the *Fendrr* lncRNA to the genome of target genes  
92   (Grote and Herrmann, 2013). To address if this region is required for *Fendrr* function, we  
93   deleted this *FendrrBox* (*Fendrr*<sup>em7Phg/em7Phg</sup>) in mouse embryonic stem cells (mESCs)  
94   (Figure 1A). We generated embryos from these mESCs and compared them to the *Fendrr*  
95   null phenotype (Figure 1B). The *FendrrNull* (*Fendrr*<sup>3xpA/3xpA</sup>) embryos exhibit increased  
96   lethality starting at the embryonic stage E12.5 and all embryos were dead prior to birth  
97   and in the process of resorption (Grote et al., 2013). In contrast, the *FendrrBox* mutants,  
98   which survived longer, displayed an onset of lethality later during development (E16.5)  
99   and some embryos survived until short before birth. The surviving embryos of the  
100   *FendrrBox* mutants were born and displayed an increased postnatal lethality (Figure 1C).  
101   This demonstrates that the *FendrrBox* element in the *Fendrr* RNA is most likely partially  
102   required for *Fendrr* function in embryo development and for postnatal survival.

103

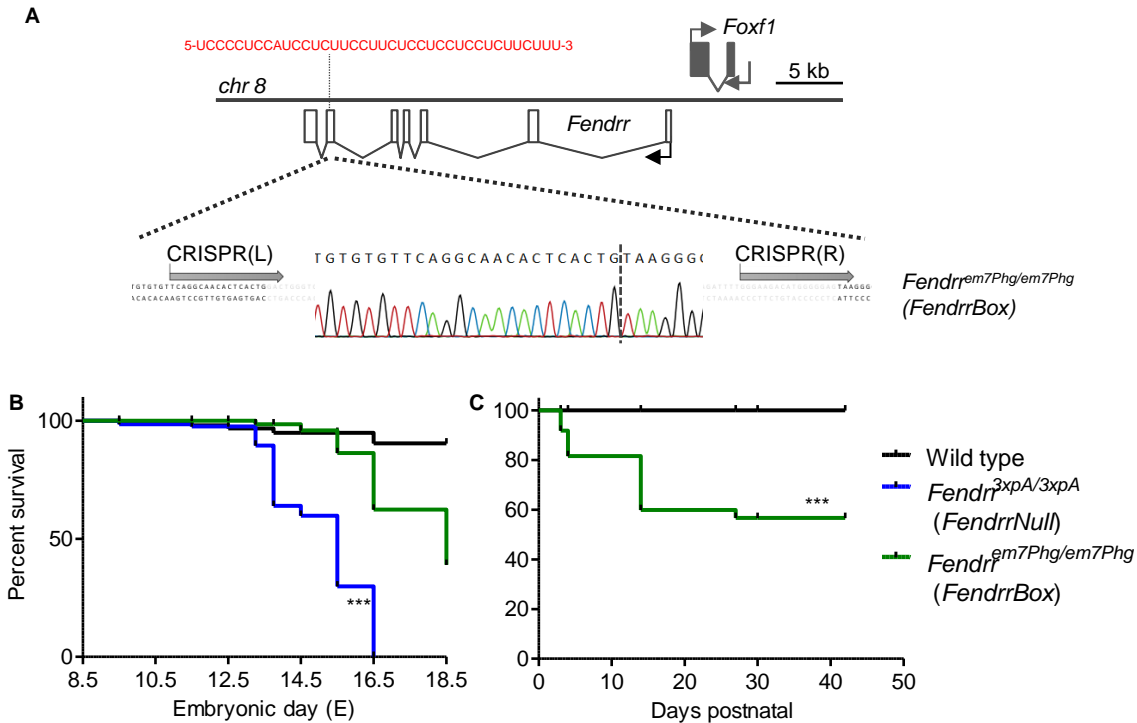


**Figure 1.** (A) Schematic of the *Fendrr* locus and the localization of the DNA interacting region (*FendrrBox*) in exon six. The localization of the gRNA binding sites (grey arrows) are indicated and the resulting deletion of 99bp, including the *FendrrBox*, in the genome that generates the *Fendrr<sup>em7Phg/em7Phg</sup>* allele (*FendrrBox*). (B) Embryos and (C) life animals were generated by tetraploid aggregation and the surviving animals counted. \*\*\* p>0.0001 by log-rank (Mantel-Cox) test

104

105

106

## Gene expression in *FendrrNull* and *FendrrBox* mutant developing lungs

107 Given the involvement of *Fendrr* in lung development (Sauvageau et al., 2013) and the  
108 involvement of mutations in human *FENDRR* in lung disease (Szafranski et al., 2013), we  
109 wanted to determine the genes affected by a loss of *Fendrr* or the *FendrrBox* in developing  
110 lungs to identify *Fendrr* target genes. However, when we collected the lungs from surviving  
111 embryos of the E14.5 stage we did not identify any significant dysregulation of genes,  
112 neither in the *FendrrNull* nor in the *FendrrBox* mutant lungs (Figure S1). One explanation  
113 is that the incomplete genetic penetrance of *Fendrr* mutants results in a compositional  
114 bias. Surviving embryos do not display any differences in gene regulation and those which  
115 did, were lethal and the embryos died already. To circumvent this issue, we collected  
116 embryonic lungs from E12.5 stage embryos, before the timepoint that any lethality occurs  
117 and cultivated the lung explants *ex vivo* under defined conditions. After 5 days of

118 cultivation some lungs from all phenotypes detached from the supporting membrane.  
119 Hence, we choose to analyze 4 day cultivated lungs (corresponding then to E16.5) (Figure  
120 2A). When we compared expression between wild type, *FendrrNull* and *FendrrBox* mutant  
121 E16.5 *ex vivo* lungs we found 119 genes dysregulated in *Fendrr null* and 183 genes in  
122 *FendrrBox* mutant lungs compared to wild type (Figure 2B). When we analyzed the GO  
123 terms of downregulated genes in both *Fendrr* mutants we found mainly genes involved in  
124 lung and respiratory system development, as well as cell-cell contact organization and  
125 extracellular matrix organization (Figure 2C). Upregulated genes in both mutants were  
126 mostly associated with genome organization, replication, and genome regulation. Overall,  
127 60 genes were commonly dysregulated in both mutants (Figure 2D). Strikingly, these  
128 shared dysregulated genes are mostly associated with lung fibrosis, a major condition of  
129 various lung disease, including idiopathic pulmonary fibrosis (IPF).

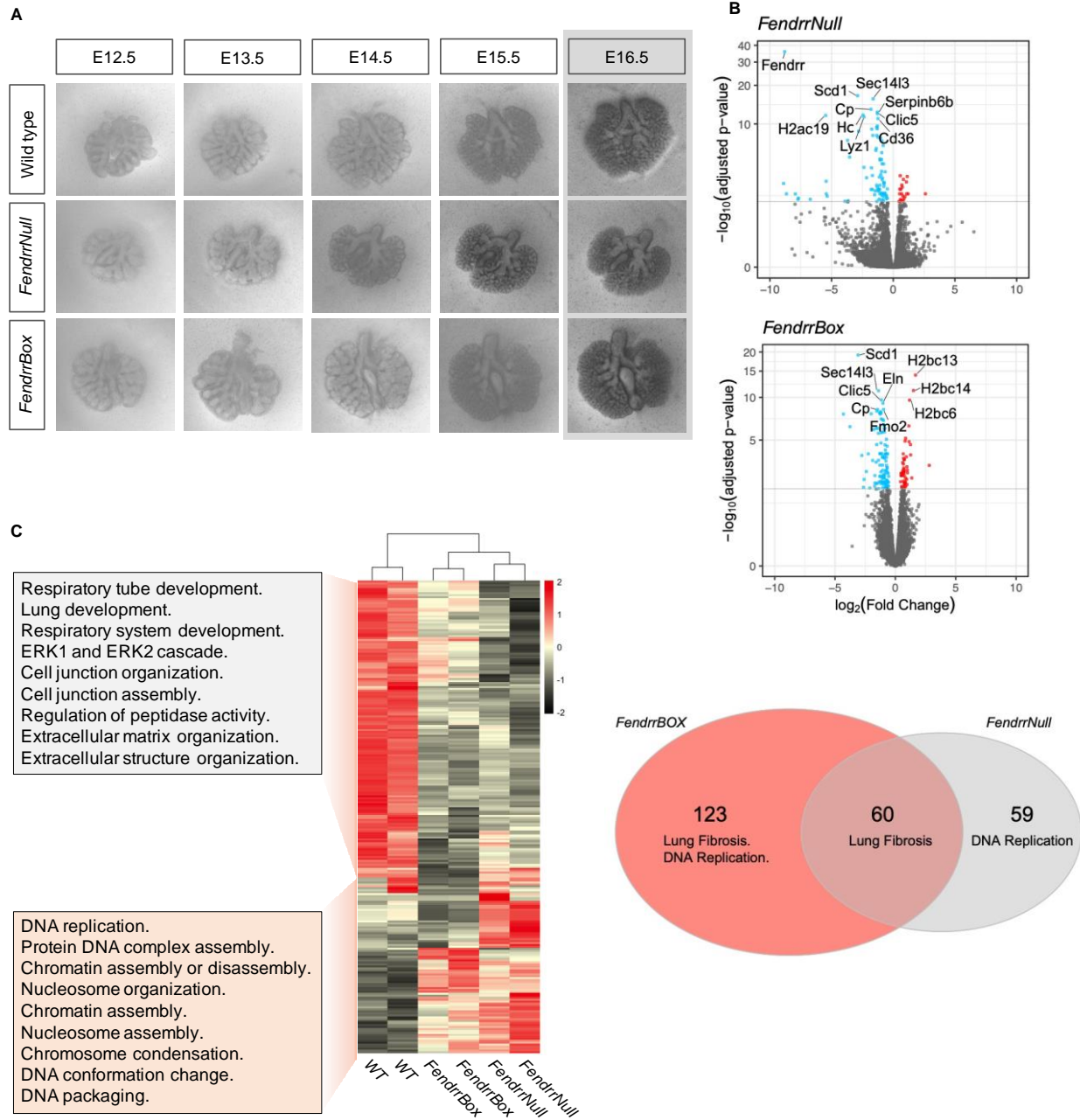


**Figure 2.** Expression profiling of *Fendrr* mutant lungs in *ex vivo* development.

(A) Representative images from a time course of *ex vivo* developing lungs from the indicated genotype. The last time point representing E16.5 of embryonic development is the endpoint and lungs were used for expression profiling. (B) Volcano plot representation of deregulated genes in the two *Fendrr* mutants determined by RNA-seq of two biological replicates. (C) Heatmap of all 242 deregulated genes of both *Fendrr* mutants compared to wild type. The GO terms of the either up- or downregulated gene clusters are given in the box as determined by topGO bioconductor package. (D) Venn diagram of the individually deregulated genes and the overlap in the two different *Fendrr* mutants. Pathway analysis performed by wikiPathways is given for each DE genes cluster.

130

131



## 132 **RNA:dsDNA triplex target genes in fibrosis**

133 It is conceivable that some of these dysregulated genes are primary targets of *Fendrr* and  
134 some represent secondary targets. To identify which of these dysregulated genes in  
135 *Fendrr* mutant lungs are likely to be direct targets of *Fendrr* via its triplex forming  
136 *FendrrBox*, we used the Triplex Domain Finder (TDF) algorithm (Kuo et al., 2019) to  
137 identify triplex forming sites on *Fendrr* within the promoters of the dysregulated target  
138 genes. The single significant triplex forming site (or DBD = DNA Binding Domain)  
139 discovered by TDF is the *FendrrBox* (Figure 1A, 3A), confirming previous results. The  
140 TDF algorithm didn't identify significant binding of *Fendrr* to target promoters in either  
141 *FendrrBox* exclusive nor the *FendrrNull* exclusive dysregulated genes. However, the TDF  
142 algorithm detects a significant *FendrrBox* binding site in promoters of 20 out of the 60  
143 target genes from the overlapping gene set of *FendrrBox* and *FendrrNull* mutants (Fig  
144 3A). The *FendrrBox* binding element (BE) in these 20 genes is a non-perfect match  
145 (Figure 3B) for those target genes. We refer to these genes as direct *FendrrBox* target  
146 genes and most of these 20 genes are downregulated in loss of function *Fendrr* mutants  
147 (Figure 3C). When we analyzed more closely the GO terms associated with these shared  
148 genes, we find most terms to be associate with cell adhesion and extracellular matrix  
149 functions, a typical hallmark for fibrosis, where collagen and related components are  
150 deposited from cells.

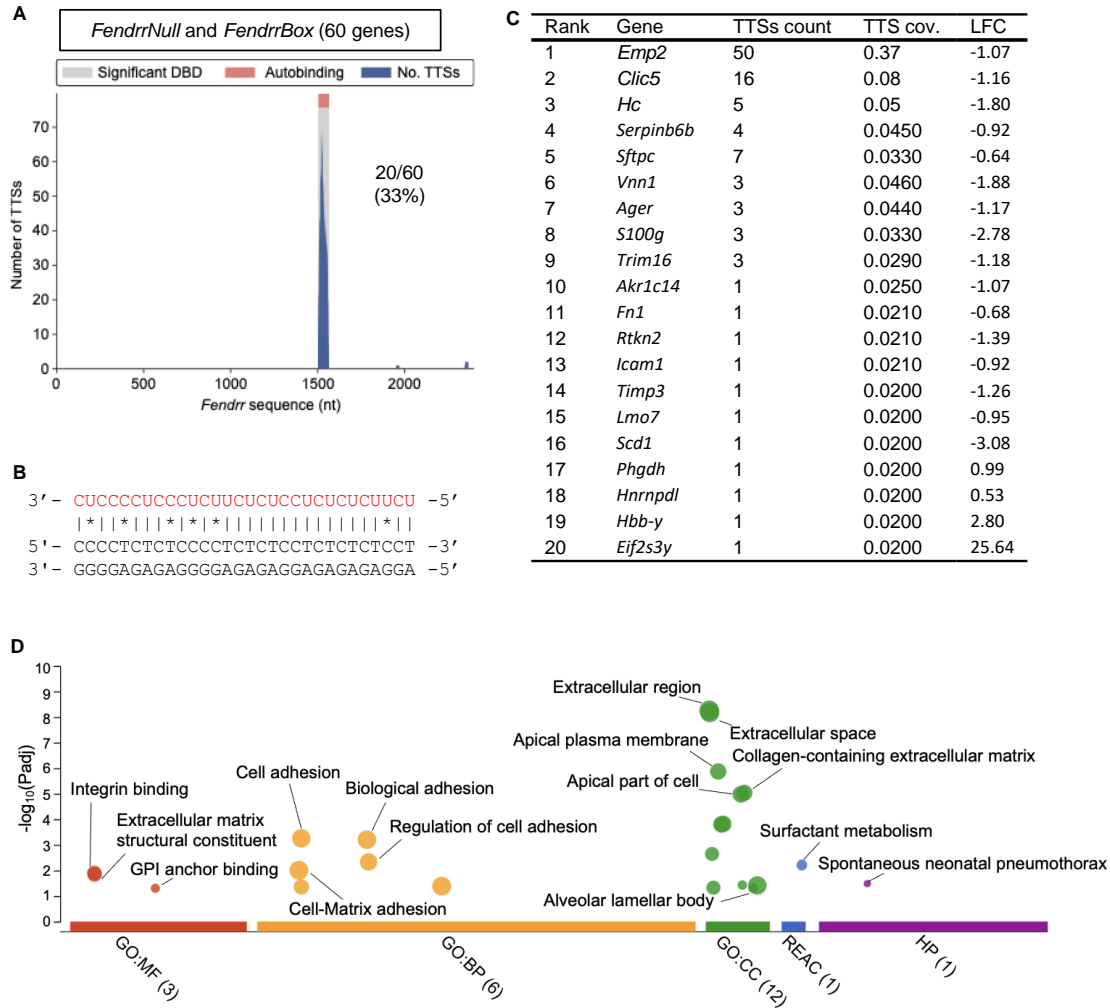


Figure 3. Potential direct target genes of *Fendrr*.

(A) Triplexes analysis of the 60 shared dysregulated genes identifies 20 genes with a potential *Fendrr* triplex interacting site at their promoter. DBD = DNA Binding Domain on RNA, TTS = triple target DNA site. (B) Representation of the *Fendrr* triplex (red) RNA sequence and a typical genomic binding element at *Emp2* promoter. (C) List of the 20 *Fendrr* target genes that depend on the *Fendrr* triplex and have a *Fendrr* binding site at their promoter. (D) Functional profiling analysis of these 20 genes. MF= molecular function, BP = biological process, CC = cellular component, Reactome (Reac), and Human pathways (HP) analysis. The size of each bubble represents the number of genes from the 20 genes that are involved in the enriched ontology.

151

## 152 Signaling dependent regulation by *Fendrr*

153 To functionally test for direct *Fendrr* targets, we wanted to analyze the expression of these  
 154 20 genes in NIH3T3 mouse fibroblasts. Only 6 out of these 20 are expressed in this cell  
 155 line and *Fendrr* is only very lowly expressed. To activate endogenous *Fendrr* expression  
 156 we tested several gRNAs to recruit the dCAS9-SAM transcriptional activator complex  
 157 (Konermann et al., 2014) to the promoter region of *Fendrr*. We identified three gRNAs  
 158 (Figure 4A) that could exclusively activate endogenous *Fendrr* without significant

159 activation of the *Foxf1* gene (Figure 4B). Such transfected fibroblasts have a 15-fold  
 160 increase in *Fendrr* transcript. Upon over activation of endogenous *Fendrr*, none of the  
 161 expressed *FendrrBox* target genes displayed an increase in expression (Figure 4C), as it  
 162 would be expected as these genes are downregulated in *Fendrr* loss-of-function mutants  
 163 (Figure 3C). We speculated that in addition to overexpression of *Fendrr*, an additional  
 164 pathway needs to be activated. The BMP, FGF and Wnt pathway are known to play an  
 165 important role in lung fibrosis (Cassandras et al., 2020; Hosseinzadeh et al., 2018). We  
 166 therefore activated the BMP signaling pathway, FGF-signaling pathway and the Wnt  
 167 signaling pathway in these fibroblasts. We found that only when Wnt signaling was  
 168 activated, overactivation of *Fendrr* could increase the expression of nearly all the  
 169 expressed *FendrrBox* target genes. This places the lncRNA *Fendrr* as a direct co-activator  
 170 of Wnt-signaling in fibroblasts and most likely in lung fibrosis.

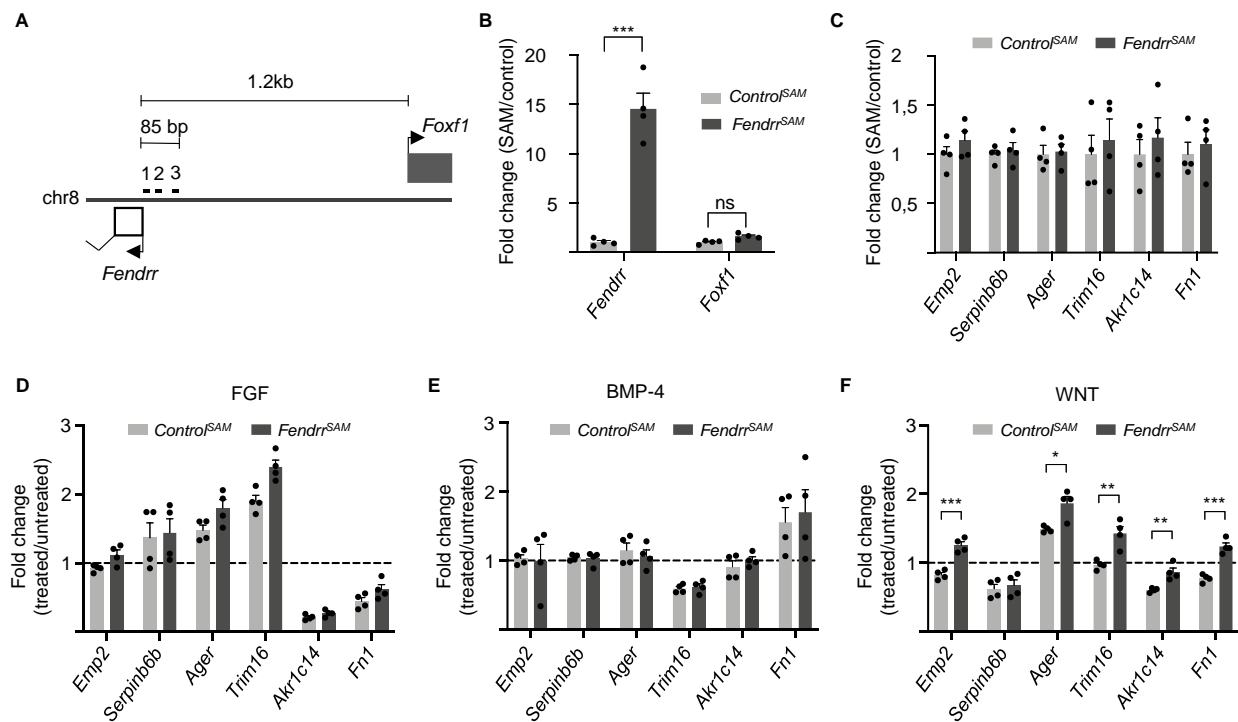


Figure 4. Wnt-dependent *Fendrr* target gene regulation

(A) Schematic of the *Foxf1* and *Fendrr* promoter region with the indication of the location of the 3 gRNAs used for specific *Fendrr* endogenous activation. (B) Increase of *Fendrr* expression in NIH3T3 cells upon CRISPRa with a pool of 3 gRNAs. (C) *Fendrr* Triplex containing *Fendrr* target genes expressed in NIH3T3 cells after 48h of *Fendrr* CRISPRa (*Fendrr*<sup>SAM</sup>). (D) Expression changes after 48hrs of co-stimulation with FGF. (E) Expression changes after 48hrs of co-stimulation with BMP-4. (F) Expression changes after 48hrs of co-stimulation with WNT. The dashed line represent the normalised expression value (set to 1) of the untreated cells transfected with control gRNA. (D-F) Statistics are given when significance by t-test analysis.

172 **Discussion**

173 We showed previously that *Fendrr* can bind to promoters of target genes in the lateral  
174 plate mesoderm of the developing mouse embryo (Grote and Herrmann, 2013; Grote et  
175 al., 2013). As *Fendrr* can also bind to histone modifying complexes, it is assumed that  
176 *Fendrr* directs these complexes to its target genes. However, that the *FendrrBox* might be  
177 the recruiting element was so far only supported by a biochemical approach that shows  
178 binding of the *FendrrBox* RNA element to two target promoters *in vitro* (Grote et al., 2013).

179 The involvement of *Fendrr* in lung formation was shown previously, albeit with a  
180 completely different approach to the removal of *Fendrr*. The replacement of the full length  
181 *Fendrr* locus by a *lacZ* coding sequence resulted in homozygous postnatal mice to stop  
182 breathing within 5h after birth (Sauvageau et al., 2013). These mice also allowed for  
183 tracing *Fendrr* expression to the pulmonary mesenchyme, to which also vascular  
184 endothelial cells and fibroblasts belong. At the E14.5 stage *FendrrLacZ* mutant mice  
185 exhibit hypoplastic lungs. Our *ex vivo* analysis of lungs from our specific *Fendrr* mutants  
186 confirms the involvement of *Fendrr* in lung development. Here we show for the first time  
187 that the *FendrrBox* is at least partially required for *in vivo* functions of *Fendrr* and identified  
188 several, potential direct target genes of *Fendrr* in lung development. Moreover, the  
189 analysis of the dysregulated genes in the two different mouse mutant lungs indicates, that  
190 specifically *Fendrr* in the fibroblast might play an important role.

191 Studying embryonic development of the lung and its comparison to idiopathic lung fibrosis  
192 (IPF) in the adult lung has revealed that many of the same gene networks are in place to  
193 regulate both processes (Shi et al., 2009). A multitude of different signaling pathway are  
194 implicated in IPF (Hosseinzadeh et al., 2018). A prime example for an important pathway  
195 in IPF is the Wnt signaling pathway (Baarsma and Königshoff, 2017) and, in particular,  
196 increased Wnt signaling is associated with IPF and, hence, inhibition of Wnt signaling  
197 counteracts fibrosis (Cao et al., 2018). While the contribution of developmental signaling  
198 pathways to IPF is well understood, the contribution of lncRNAs in IPF is just beginning to  
199 be addressed (Hadjicharalambous and Lindsay, 2020). In humans, it was shown that in  
200 IPF patients *FENDRR* is increased in lung tissue (Huang et al., 2020). Intriguingly, in  
201 single cell RNA-seq approaches from human lung explants, *FENDRR* is highly expressed  
202 in vascular endothelial (VE) cells, but also significantly expressed in fibroblasts (Adams et

203 al., 2020). Moreover, *FENDRR* expression increases in VE and in fibroblasts in IPF  
204 (Adams et al., 2020; Morse et al., 2019). It was shown recently, that *Fendrr* can regulate  
205  $\beta$ -catenin levels in lung fibroblasts (Senavirathna et al., 2021). Our data supports that Wnt  
206 signaling together with *Fendrr* is involved in target gene regulation and that *Fendrr* is a  
207 positive co-regulator of Wnt signaling in fibroblasts. This contrasts with the role of *Fendrr*  
208 in the precursor cells of the heart, the lateral plate mesoderm. Loss of *Fendrr* function  
209 results in the upregulation of *Fendrr* target genes, establishing that *Fendrr* is a suppressor  
210 of gene expression. The finding that *Fendrr* can act as either a suppressor or an activator  
211 of transcription, depending on the cell type, highlights the crosstalk between lncRNAs and  
212 signaling pathway, which broadens our understanding of the versatility of lncRNA in the  
213 cellular functions.

214

215

216

### 217 **Acknowledgements**

218 We thank Dijana Micic for excellent animal husbandry and Karol Macura for the generation  
219 of the transgenic mice. We want to thank Heiner Schrewe for help with *ex vivo* culture of  
220 embryonic lungs. This research was funded by the DFG (German Research Foundation)  
221 Excellence Cluster Cardio-Pulmonary System (Exc147-2) and a DFG research grant GR  
222 4745/1-1 to P.G. T.A and S.R. are supported by the TRR267 of the DFG.

223

224

225

### 226 **Competing interests**

227 The authors declare no competing interest.

228

## 229 Literature

- 230 Adams, T.S., Schupp, J.C., Poli, S., Ayoub, E.A., Neumark, N., Ahangari, F., Chu, S.G., Raby, B.A., Deluiliis,  
231 G., Januszyk, M., et al. (2020). Single-cell RNA-seq reveals ectopic and aberrant lung-resident cell  
232 populations in idiopathic pulmonary fibrosis. *Sci. Adv.* *6*, eaba1983.
- 233 Ali, T., and Grote, P. (2020). Beyond the RNA-dependent function of lncRNA genes. *Elife* *9*.
- 234 Baarsma, H.A., and Königshoff, M. (2017). “WNT-er is coming”: WNT signalling in chronic lung diseases.  
235 *Thorax* *72*, 746–759.
- 236 Cao, H., Wang, C., Chen, X., Hou, J., Xiang, Z., Shen, Y., and Han, X. (2018). Inhibition of Wnt/ $\beta$ -catenin  
237 signaling suppresses myofibroblast differentiation of lung resident mesenchymal stem cells and  
238 pulmonary fibrosis. *Sci. Rep.* *8*, 1–14.
- 239 Cassandras, M., Wang, C., Kathiriya, J., Tsukui, T., Matatia, P., Matthay, M., Wolters, P., Molofsky, A.,  
240 Sheppard, D., Chapman, H., et al. (2020). Gli1+ mesenchymal stromal cells form a pathological niche to  
241 promote airway progenitor metaplasia in the fibrotic lung. *Nat. Cell Biol.* *22*, 1295–1306.
- 242 Gong, L., Zhu, L., and Yang, T. (2020). Fendrr involves in the pathogenesis of cardiac fibrosis via regulating  
243 miR-106b/SMAD3 axis. *Biochem. Biophys. Res. Commun.* *524*, 169–177.
- 244 Grote, P., and Herrmann, B.G. (2013). The long non-coding RNA Fendrr links epigenetic control  
245 mechanisms to gene regulatory networks in mammalian embryogenesis. *RNA Biol.* *10*, 1579–1585.
- 246 Grote, P., Wittler, L., Hendrix, D., Koch, F., Währisch, S., Beisaw, A., Macura, K., Bläss, G., Kellis, M.,  
247 Werber, M., et al. (2013). The tissue-specific lncRNA Fendrr is an essential regulator of heart and body  
248 wall development in the mouse. *Dev. Cell* *24*, 206–214.
- 249 Hadjicharalambous, M.R., and Lindsay, M.A. (2020). Idiopathic pulmonary fibrosis: Pathogenesis and the  
250 emerging role of long non-coding RNAs. *Int. J. Mol. Sci.* *21*, 1–19.
- 251 Herriges, M.J., Swarr, D.T., Morley, M.P., Rathi, K.S., Peng, T., Stewart, K.M., and Morrissey, E.E. (2014).  
252 Long noncoding RNAs are spatially correlated with transcription factors and regulate lung development.  
253 *Genes Dev.* *28*, 1363–1379.
- 254 Hon, C.C., Ramilowski, J.A., Harshbarger, J., Bertin, N., Rackham, O.J.L., Gough, J., Denisenko, E.,  
255 Schmeier, S., Poulsen, T.M., Severin, J., et al. (2017). An atlas of human long non-coding RNAs with  
256 accurate 5' ends. *Nature* *543*, 199–204.
- 257 Hosseinzadeh, A., Javad-Moosavi, S.A., Reiter, R.J., Hemati, K., Ghaznavi, H., and Mehrzadi, S. (2018).  
258 Idiopathic pulmonary fibrosis (IPF) signaling pathways and protective roles of melatonin. *Life Sci.* *201*,  
259 17–29.
- 260 Huang, C., Liang, Y., Zeng, X., Yang, X., Xu, D., Gou, X., Sathiaselan, R., Senavirathna, L.K., Wang, P., and  
261 Liu, L. (2020). Long noncoding RNA FENDRR exhibits antifibrotic activity in pulmonary fibrosis. *Am. J.*  
262 *Respir. Cell Mol. Biol.* *62*, 440–453.
- 263 Konermann, S., Brigham, M.D., Trevino, A.E., Joung, J., Abudayyeh, O.O., Barcena, C., Hsu, P.D., Habib, N.,  
264 Gootenberg, J.S., Nishimasu, H., et al. (2014). Genome-scale transcriptional activation by an engineered  
265 CRISPR-Cas9 complex. *Nature* *517*, 583–588.
- 266 Kuo, C.C., Hänzelmann, S., Sentürk Cetin, N., Frank, S., Zajzon, B., Derks, J.P., Akhade, V.S., Ahuja, G.,  
267 Kanduri, C., Grummt, I., et al. (2019). Detection of RNA-DNA binding sites in long noncoding RNAs.  
268 *Nucleic Acids Res.* *47*.

- 269 Li, Y., Syed, J., and Sugiyama, H. (2016). RNA-DNA Triplex Formation by Long Noncoding RNAs. *Cell Chem.*  
270 *Biol.* *23*, 1325–1333.
- 271 Mahlapuu, M., Ormestad, M., Enerbäck, S., and Carlsson, P. (2001). The forkhead transcription factor  
272 Foxf1 is required for differentiation of extra-embryonic and lateral plate mesoderm. *Development* *128*,  
273 155–166.
- 274 Melissari, M.-T., and Grote, P. (2016). Roles for long non-coding RNAs in physiology and disease. *Pflügers*  
275 *Arch.* *468*, 945–958.
- 276 Morse, C., Tabib, T., Sembrat, J., Buschur, K.L., Bittar, H.T., Valenzi, E., Jiang, Y., Kass, D.J., Gibson, K.,  
277 Chen, W., et al. (2019). Proliferating SPP1/MERTK-expressing macrophages in idiopathic pulmonary  
278 fibrosis. *Eur. Respir. J.* *54*.
- 279 Polack, F.P., Thomas, S.J., Kitchin, N., Absalon, J., Gurtman, A., Lockhart, S., Perez, J.L., Pérez Marc, G.,  
280 Moreira, E.D., Zerbini, C., et al. (2020). Safety and Efficacy of the BNT162b2 mRNA Covid-19 Vaccine. *N.*  
281 *Engl. J. Med.* *383*, 2603–2615.
- 282 Sauvageau, M., Goff, L. a, Lodato, S., Bonev, B., Groff, A.F., Gerhardinger, C., Sanchez-Gomez, D.B.,  
283 Haciosuleyman, E., Li, E., Spence, M., et al. (2013). Multiple knockout mouse models reveal lincRNAs are  
284 required for life and brain development. *Elife* *2*, e01749.
- 285 Senavirathna, L.K., Liang, Y., Huang, C., Yang, X., Bamunuarachchi, G., Xu, D., Dang, Q., Sivasami, P.,  
286 Vaddadi, K., Munteanu, M.C., et al. (2021). Long noncoding rna fendrr inhibits lung fibroblast  
287 proliferation via a reduction of  $\beta$ -catenin. *Int. J. Mol. Sci.* *22*.
- 288 Shi, W., Xu, J., and Warburton, D. (2009). Development, repair and fibrosis: What is common and why it  
289 matters series. *Respirology* *14*, 656–665.
- 290 Stankiewicz, P., Sen, P., Bhatt, S.S., Storer, M., Xia, Z., Bejjani, B. a, Ou, Z., Wiszniewska, J., Driscoll, D.J.,  
291 Maisenbacher, M.K., et al. (2009). Genomic and genic deletions of the FOX gene cluster on 16q24.1 and  
292 inactivating mutations of FOXF1 cause alveolar capillary dysplasia and other malformations. *Am. J. Hum.*  
293 *Genet.* *84*, 780–791.
- 294 Szafranski, P., Dharmadhikari, A. V, Brosens, E., Gurha, P., Kolodziejska, K.E., Zhishuo, O., Dittwald, P.,  
295 Majewski, T., Mohan, K.N., Chen, B., et al. (2013). Small noncoding differentially methylated copy-  
296 number variants, including lincRNA genes, cause a lethal lung developmental disorder. *Genome Res.* *23*,  
297 23–33.
- 298 Xiao, J.-H., Hao, Q.-Y., Wang, K., Paul, J., and Wang, Y.-X. (2017). Emerging Role of MicroRNAs and Long  
299 Noncoding RNAs in Healthy and Diseased Lung. pp. 343–359.
- 300 Yu, S., Shao, L., Kilbride, H., and Zwick, D.L. (2010). Haploinsufficiencies of FOXF1 and FOXC2 genes  
301 associated with lethal alveolar capillary dysplasia and congenital heart disease. *Am. J. Med. Genet. A*  
302 *152A*, 1257–1262.
- 303
- 304

## 305 **EXPERIMENTAL PROCEDURES**

306

### 307 **Culturing of mouse ES cells**

308 The mESC were either cultured in feeder free 2i media or on feeder cells (mitomycin inactivated  
309 SWISS embryonic fibroblasts) containing LIF1 (1000 U/ml). 2i media: 1:1 Neurobasal (Gibco  
310 #21103049) :F12/DMEM (Gibco #12634-010), 2 mM L-glutamine (Gibco), 1x Penicillin/  
311 Streptomycin (100x penicillin (5000 U/ml,) / streptomycin (5000ug/ml), Sigma #P4458-100ML, 2  
312 mM glutamine (100x GlutaMAX™ Supplement, Gibco #35050-038), 1x non-essential amino acids  
313 (100x MEM NEAA, Gibco #11140-035), 1x Sodium pyruvate (100x, Gibco, #11360-039), 0.5x B-  
314 27 supplement, serum-free (Gibco # 17504-044), 0.5x N-2 supplement (Gibco # 17502-048),  
315 Glycogen synthase kinase 3 Inhibitor (GSK-Inhibitor, Sigma, # SML1046-25MG), MAP-Kinase  
316 Inhibitor (MEK-Inhibitor Sigma, #PZ0162), 1000 U/ml Murine\_Leukemia\_Inhibitory\_Factor  
317 ESGRO (10<sup>7</sup> LIF, Chemicon #ESG1107), ES-Serum media: Knockout Dulbecco's Modified  
318 Eagle's Medium (DMEM Gibco#10829-018), ES cell tested fetal calf serum (FCS), 2 mM  
319 glutamine, 1x Penicillin/ Streptomycin, 1x non-essential amino acids, 110 nM β-Mercaptoethanol,  
320 1x nucleoside (100x Chemicon #ES-008D), 1000 U/ml LIF1.

321 The cells were split with TrypLE Express (1x, Gibco #12605-010) and the reaction was stopped  
322 with the same amount of Phosphate-Buffered Saline (PBS Gibco #100100239) followed by  
323 centrifugation at 1000 rpm for 5min. The cells were frozen in the appropriate media containing  
324 10% Dimethyl sulfoxide (DMSO, Sigma Aldrich #D5879). To minimize any effect of the 2i (Choi et  
325 al., 2017) on the developmental potential mESC were only kept in 2i for the antibiotic selection  
326 after transient transfection with CRISPR/Cas9 or mini gene integration and DNA generation for  
327 genotyping. At all other times cells were maintained on ES-Serum media on feeder cells.

328

### 329 **Generation of transgenic or CRISPR/Cas9 edited mESC**

330 Guide RNAs were designed, using the [crispr.mit.edu](http://crispr.mit.edu) website with the nickase option. The  
331 following, top-scoring guide RNAs were selected and cloned into pX330 (Addgene, # 42230)  
332 plasmid to allow for transient puromycin selection after transfection. The sgRNAs used for the  
333 deletion of the FendrrBox are upstream(L): TCAGGCAACACTCACTGGAC, downstream(R):  
334 GGGAAGACATGGGGGAGTAA. Wild-type F1G4 cells were transiently transfected with 2μg/mL  
335 puromycin (Gibco, #10130127) for 2 days and 1μg/mL puromycin for 1 day. Single mESC clones  
336 were picked 7-8 days after transfection and plated onto 96-well synthemax (Sigma, #CLS3535)



337 coated plates and screened for genomic DNA deletion by PCR using primers outside of the  
338 deletion region.

339

#### 340 **Genotyping of *Fendrr*<sup>3xpA/3xpA</sup> and *Fendrr*<sup>em7Phg/em7Phg</sup> tissues**

341 The REExtract-N-Amp™ Tissue PCR Kit (Merck, XNAT) was used for genotyping for all tissue  
342 explants. Genotyping of *FendrrNull* (*Fendrr*<sup>3xpA/3xpA</sup>) embryos with the three primers:  
343 *Fendrr*3xpA\_F1: GCGCTCCCCACTCACGTTCC, *Fendrr*3xpA\_Ra1:  
344 AGGTTCTTCACAAAGATCCCAAGC, genoNCrna\_Ra4:  
345 AAGATGGGGAACCGAGAATCCAAAG that will generate a 696bp band in wild type and a 371bp  
346 band when the 3xpA allele is present. Genotyping of *FendrrBox* (*Fendrr*<sup>em7Phg/em7Phg</sup>) embryo  
347 tissues with: *Fendrr*Box\_F2: ATGCTTCCAAGGAAGGACGG, *Fendrr*Box\_R2:  
348 CTTGACGCCAAGCTCCTGTA that generate a 602bp product in wild type and a 503bp product  
349 when the *FendrrBox* is missing.

350

#### 351 **Lung preparation and RNA isolation**

352 Staged embryo lungs were dissected from uteri into PBS and kept on ice in M2 media (Merck,  
353 M7167-50ML) until further processing. For direct RNA isolation the lung tissue was transferred  
354 into Precellys beads CK14 tubes (VWR, 10144-554) containing 1ml 900 µl Qiazol (Qiagen,  
355 #79306) and directly processed with a Bertin Minilys personal homogenizer. To remove the DNA  
356 100 µl gDNA Eliminator solution was added and 180 µl Chloroform (AppliChem, #A3633) to  
357 separate the phases. The extraction mixture was centrifuge at full speed, 4°C for 15min. The  
358 aqueous phase was mixed with the same amount of 70 % Ethanol and transferred to a micro or  
359 mini columns depending of the amount of tissue and cells. The RNA was subsequently purified  
360 with the Qiagen RNAeasy Plus Min Kit (Qiagen, #74136) according the manufacturers manual.  
361 Remaining tissue from the same embryos was used for genotyping to select homozygous mutants.

362

#### 363 **Lung ex vivo culture**

364 The lung culture was adopted from a previous published protocol (Hogan et al., 1994). Lungs were  
365 dissected from the E12.5 staged embryos in ice-cold PBS containing 0.5% FCS. Lungs were then  
366 placed in holding medium: Leibovitz's L-15 Medium (ThermoFisher Scientific, 11415064)  
367 containing 1x Corning™ MITO+ Serum Extender (Fisher scientific, 10787521) and 1x Pen/Strep.

368 Explant media (Advanced DMEM/F12 (ThermoFisher Scientific, 12634010), 5x Corning™ MITO+  
369 Serum Extender, 1x Pen/Strep, 10% FCS) was placed into a 6-well tissue culture dish (0.8-1.0ml)  
370 and the 6-well plate fitted with Falcon™ Cell Culture Inserts with 8 um pore size (Fisher Scientific,  
371 08-771-20). The lungs were transferred from the holding medium onto the membrane with a sterile  
372 razor blade and 5-10 ul of holding media to keep the lungs wet. Cells were cultured at 37C with  
373 an atmospheric CO<sub>2</sub> of 7.5%. After the indicated time the lungs were removed from the membrane  
374 and RNA isolated as described above.

375

### 376 **Generation of mouse embryos from mESCs**

377 All animal procedures were conducted as approved by local authorities (LAGeSo Berlin) under  
378 the license number G0368/08. Embryos were generated by tetraploid morula aggregation of  
379 embryonic stem cells as described in (George et al., 2007). SWISS mice were used for either wild-  
380 type donor (to generate tetraploid morula) or transgenic recipient host (as foster mothers for  
381 transgenic mutant embryos). All transgenic embryos and mESC lines were initially on a hybrid  
382 F1G4 (C57Bl6/129S6) background and backcrossed seven times to C57Bl6J for the preparations  
383 of embryonic lungs.

384

### 385 **Real-time quantitative PCR analysis**

386 Quantitative PCR (qPCR) analysis was carried out on a StepOnePlus™ Real-Time PCR System  
387 (Life Technologies) using Fast SYBR™ Green Master Mix (ThermoFisher Scientific #4385612).  
388 RNA levels were normalized to housekeeping gene. Quantification was calculated using the  $\Delta\Delta C_t$   
389 method (Muller et al., 2002). *Rpl10* served as housekeeping control gene for qPCR. The primer  
390 concentration for single a single reaction was 250nM. Error bars indicate the standard error from  
391 biological replicates, each consisting of technical triplicates. The Oligonucleotides for the qPCRs  
392 are as follows: Emp2\_qPCR\_fw: GCTTCTCTGCTGACCTCTGG, Emp2\_qPCR\_rv:  
393 CGAACCTCTCTCCCTGCTTG, Serpinb6b\_qPCR\_fw: ATAAGCGTCTCCTCAGCCCT,  
394 Serpinb6b\_qPCR\_rv: CTTTTCCCCGAAGAGCCTGT, Trim16\_qPCR\_fw:  
395 CCACACCAGGAGAACAGCAA, Trim16\_qPCR\_rv: AGGTCCAACACTGCATACACCG,  
396 Fn1\_qPCR\_fw: GAGTAGACCCCAGGCACCTA, Fn1\_qPCR\_rv: GTGTGCTCTCCTGGTTCTCC,  
397 Akr1c14\_qPCR\_fw: TGGTCACTTCATCCCTGCAC, Akr1c14\_qPCR\_rv:  
398 GCCTGGCCTACTTCCTCTTC, Ager\_qPCR\_fw: TGGTCAGAACATCACAGCCC,  
399 Ager\_qPCR\_rv: CATTGGGGAGGATTTCGAGCC, Fendrr\_qPCR\_fw:

400 CTGCCCGTGTGGTTATAATG, Fendrr\_qPCR\_rv: TGA CTCTCAAGTGGGTGCTG,  
401 Foxf1\_qPCR\_fw: CAAAACAGTCACAACGGGCC, Foxf1\_qPCR\_rv:  
402 GCCTCACCTCACATCACACA, Rpl10\_qPCR\_fw: GCTCCACCCTTTCCATGTCA,  
403 Rpl10\_qPCR\_rv: TGCAACTTGGTTCGGATGGA.

404

#### 405 **Sequencing and analysis of RNA-seq**

406 RNA was treated to deplete rRNA using Ribo-Minus technology. Libraries were prepared from  
407 purified RNA using ScriptSeq™ v2 and were sequenced on an Illumina HiSeq platform. We  
408 obtained 60 million paired-end reads of 50 bp length. Read mapping was done with STAR aligner  
409 using default settings with the option --outSAMtype BAM SortedByCoordinate (Dobin et al., 2013)  
410 with default settings. For known transcript models we used GRCm38.100 Ensembl annotations  
411 downloaded from Ensembl repository (Zerbino et al., 2018). Counting reads over gene model was  
412 carried out using GenomicFeatures Bioconductor package (Lawrence et al., 2013). The aligned  
413 reads were analyzed with custom R scripts in order to obtain gene expression measures. For  
414 normalization of read counts and identification of differentially expressed genes we used DESeq2  
415 with Padj < 0.01 cutoff (Love et al., 2014). GO term and KEGG pathways were analyzed using  
416 g:Profiler (Raudvere et al., 2019). The data are deposited to GEO and can be downloaded under  
417 the accession number GSE186703.

418

#### 419 **Triplex prediction**

420 To calculate *Fendrr* triplex targets, DE genes from *FendrrNull* and *FendrrBox* RNA-Seq  
421 output were intersected and RNA-DNA triplex forming potential of the shared genes were  
422 calculated with Triplex Domain Finder (TDF) algorithm (Kuo et al., 2019). The command  
423 was executed with promotertest option and --organism = mm10. The rest of the options  
424 were set to the default settings.

425

#### 426 **Culturing of NIH3T3 cells**

427 NIH3T3 cells were cultured in DMEM (Gibco #11960-044) containing 10% Bovine Serum (Fisher  
428 Scientific #11510526), 1% GlutaMAX™ (Gibco #35050-038) and 1% Penicillin-Streptomycin  
429 (Sigma Aldrich #P4458). For the experiment, the cells were detached using Trypsin-EDTA (Gibco  
430 #25300-054). The reaction was stopped by adding double the amount of fresh media followed by  
431 centrifugation at 1000 rpm for 4 min. The pellet was resuspended in fresh medium and counted

432 using a Chemometec NucleoCounter NC-200 Automated Cell Counter (Wotol #2194080-18). 0.15  
433  $\times 10^6$  cells were seeded per well (Greiner Bio-One™ #657160).

434

#### 435 **CRISPR-activation of *Fendrr* and treatment of NIH3T3 cells**

436 Three guide RNAs targeting the *Fendrr* promoter were designed using the [crispor.tefor.net](http://crispor.tefor.net) website  
437 (Concordet and Haeussler, 2018). *Fendrr\_sg1*: GGCCTCCGACGCTGCGCGCC, *Fendrr\_sg2*:  
438 TCAACGTAAACACGTTCCGG, *Fendrr\_sg3*: AGTTGGCCTGATGCCCTAT. A non-specific  
439 guide RNA *ctrl\_sg*: GGGTCTTCGAGAAGACCT served as control. The guide RNAs were cloned  
440 into the sgRNA(MS2) plasmid (addgene #61424). The CRISPR SAM plasmid (pRP[Exp]-Puro-  
441 CAG-dCAS9-VP64:T2A:MS2-p65-HSF1) was a gift from Mohamed Nemir from the Experimental  
442 Cardiology Unit Department of Medicine University of Lausanne Medical School.

443 For transfection, Lipofectamine 3000 (Invitrogen #L3000001) was used following the  
444 manufacturer's guidelines. Briefly, 1  $\mu$ g total plasmid DNA (1:3 SAM to gRNA ratio) was diluted in  
445 Opti-MEM (Gibco #31985062) and mixed with p3000 reagent. Lipofectamine reagent was diluted  
446 in Opti-MEM and subsequently added to the DNA mixture. During the incubation the cells were  
447 washed with DPBS (Gibco #14190250) and provided with fresh Opti-MEM. Transfection mix was  
448 added to the cells and incubated for 4h at 37 °C. After the incubation, the media was changed  
449 with full media containing FGF (10 ng/ml bFGF, Sigma Aldrich #F0291; 25 ng/ml rhFGF, R&D  
450 Systems #345-FG), BMP-4 (40 ng/ml, R&D Systems #5020-BP-010) or CHIR99021 (3  $\mu$ M,  
451 Stemcell #72052). The treatment was replenished by changing media after 24h, cells were  
452 harvested for RNA isolation after 48h.

453

454